Clays and Clay Minerals, Vol. 48, No. 3, 392–399, 2000.

INTERCALATION CHARACTERISTICS OF 1,1′-DIETHYL-2,2′-CYANINE AND OTHER CATIONIC DYES IN SYNTHETIC SAPONITE: ORIENTATION IN THE INTERLAYER

MASASHI IWASAKI,[1] MASAKI KITA,[1] KENGO ITO,[2] ATSUYA KOHNO,[1] AND KOUSHI FUKUNISHI[1]

[1]Department of Chemistry and Materials Technology, Kyoto Institute of Technology, Matsugasaki, Sakyo-ku, Kyoto 606-8585, Japan

[2]Sony Corporation, Atsugi Tec. No. 2, Atsugi-shi, Kanagawa 243-0021, Japan

Abstract—The basal spacings of complexes of saponite with five cationic dyes, 1,1′-diethyl-2,2′-cyanine, crystal violet, methylene blue, 1,1′-diethyl-2,2′-carbocyanine, and 1,1′-diethyl-2,2′-dicarbocyanine, varied with degree of saturation of each dye. At low loading of dye to saponite, each cationic dye showed nearly the same absorption spectrum in the UV-visible region as that of its dilute aqueous solution, whereas the spectrum changed distinctly at high loading. With increasing degree of dye loading, the absorption band shifted to longer wavelength for 1,1′-diethyl-2,2′-cyanine (*J* band) and to shorter wavelength for the others (*D, H* bands). On the basis of the basal spacing of each respective dye-clay complex, the orientation of the intercalated dye molecules is proposed as follows: the major plane of the cationic dye lies horizontal to the 2:1 layer surface at low loading. With increasing loading, the dye molecules interact with adjacent dye molecules and orient vertically to the 2:1 layer at high loading near the cation-exchange capacity.

Key Words—Clay-Dye Complex, Crystal Violet, Cyanine Dyes, Methylene Blue, Orientation of Dye Molecules, Saponite, Visible Spectroscopy.

INTRODUCTION

Many classes of dyes in aqueous solution often show changes in their absorption spectra when the concentration of the dye is varied. Such spectral changes are attributed to the interaction of the dye molecules that form dimers and/or higher aggregates (Duxbury, 1995). The aggregates are caused mainly by the interaction between the π-electrons of the neighboring dyes. This spectral change is called "metachromasy". Many cationic dyes, such as methylene blue, acrydine orange, and crystal violet, show a shift of absorption bands to shorter wavelength (Hypsochromic shift) upon the interaction of dye molecules to form *H*-aggregates, whereas some cyanine dyes, such as 1,1′-diethyl-2,2′-cyanine, show a shift to longer wavelength (Bathochromic shift) upon the specific interaction of dye molecules to form *J*-aggregates (Jelley, 1936) in aqueous solution. *J*-aggregation of cyanine dyes is intensively studied for photographic technology, because the interaction of dyes plays an important role in the spectral sensitization of silver halide (Carroll *et al.,* 1980).

Addition of a small amount of adsorbent to a dilute dye solution causes similar effects to those observed by increasing the concentration of dye. Presumably, the adsorbed dyes form dimers and higher aggregates at adsorption sites because the dyes are highly concentrated on the surfaces of adsorbents relative to the bulk solution. When cationic dyes are adsorbed to clays, the monomer band becomes weaker and new bands appear at shorter and/or longer wavelength in ultraviolet (UV)-visible spectra. For example, substituted porphyrins, which are trapped in interlamellar galleries of Laponite and flattened by constraint within those galleries, show a red shift in their absorption bands (Chernia and Gill, 1999). This spectral change, however, is different from the metachromasy caused by dye aggregation. Ogawa and Kuroda (1995) reviewed the intercalation of cationic dyes in clays to discuss the effect on physical and chemical properties of the dye-clay complexes. However, the orientation of dyes in the interlayer remains unclear. Only a few studies on the intercalation of cyanine dyes in clay, for example, by Ogawa *et al.* (1996), have been reported.

We investigated the intercalation of cationic dyes in synthetic saponite to develop color-image fixation in thermal-transfer printing, where the dense color of dyes markedly changes the hue (Ito *et al.,* 1994, 1996). Thus, the cause of the hue change on dye-clay fixation is being investigated for the application of full-color printing. In this study, the orientation of a series of intercalated 1,1′-diethyl-2,2′-cyanine dyes in saponite is investigated. Related cationic dyes, planar methylene blue (Hang and Brindley, 1970; Saehr *et al.,* 1978; Cenens and Schoonheydt, 1988; Schoonheydt and Heughebaert, 1992; Breen and Rock, 1994), and propeller-shaped crystal violet (Yariv *et al.,* 1990) are examined also. Models are proposed from UV-visible spectral analysis and powder X-ray diffraction data.

EXPERIMENTAL

Three cyanine dyes, 1,1′-diethyl-2,2′-cyanine chloride (CN-0), 1,1′-diethyl-2,2′-carbocyanine iodide (CN-1), and 1,1′-diethyl-2,2′-dicarbocyanine iodide (CN-2) were prepared by Hayashibara Biochemical

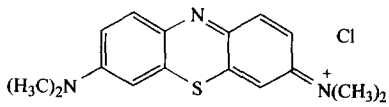

Methylene Blue (MB)

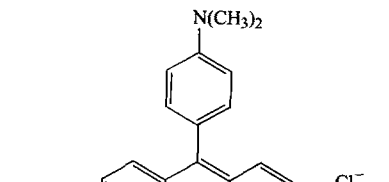

Crystal Violet (CV)

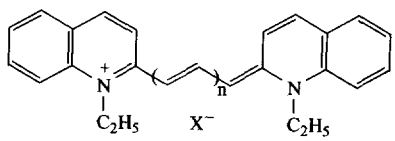

n=0, X=Cl; 1,1'-diethyl-2,2'-cyanine (CN-0)
n=1, X=I; 1,1'-diethyl-2,2'-carbocyanine (CN-1)
n=2, X=I; 1,1'-diethyl-2,2'-dicarbocyanine (CN-2)

Figure 1. Structure of the 0studied dyes.

Laboratories, Inc. (Okayama, Japan). Two other dyes, methylene blue (MB) and crystal violet (CV), were purchased in "special-grade" quality from Nakalai Tesque Inc. (Kyoto, Japan). Figure 1 shows the structures of the five dyes. The clay used here is a commercially available synthetic saponite ("SUMECTON SA") with a formula of $[(Si_{7.20}Al_{0.80})(Mg_{5.97}Al_{0.03})O_{20}(OH)_4]^{-0.77}(Na_{0.49}Mg_{0.14})^{+0.77}$ from Kunimine Industry Co. Ltd. (Tochigi, Japan). The cation-exchange capacity (CEC) is calculated at 99.7 meq/100 g-clay and MB adsorption is 132 mmol/100 g-clay on the basis of data from Kunimine.

Absorption spectra of aqueous solutions and dye-clay suspensions were measured in the visible region using a spectrophotometer, Hitachi U-3410. Aqueous solutions of CN-0, MB, and CV were used to prepare dye-clay suspensions. A solution of ethanol and water (50/50 v/v) was used for CN-1 and CN-2 because of their poor solubilities in pure water. The dye-clay suspensions were maintained at 25°C for 2 d with frequent agitation. The aqueous suspension of fine particles (<1 μm) of saponite was transparent in the visible region. After spectroscopic study of the suspensions, the supernatants were isolated by centrifugation at 10,000 rpm for 1 h, and then filtered through a 0.4-μm membrane film. No absorption in the spectra of the filtrates indicated that the total amount of added dye had adsorbed to the clay.

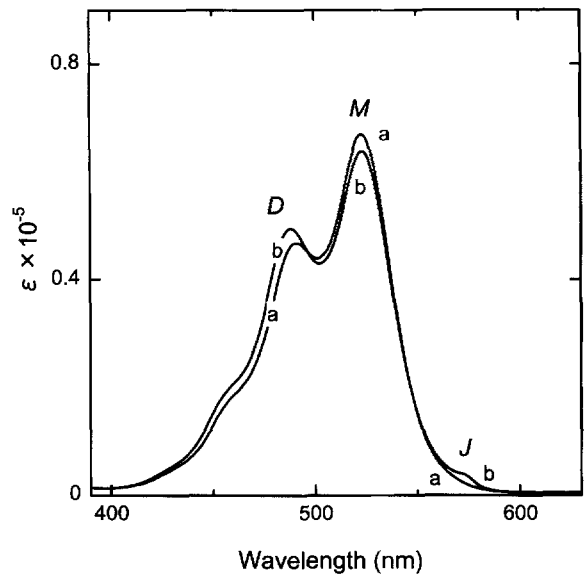

Figure 2. Absorption spectra of CN-0 in aqueous solutions. Curve (a) shows the spectrum for a concentration of 1.0×10^{-5} mol dm^{-3} and (b) for 2.0×10^{-4} mol dm^{-3}. ϵ is the molar absorption coefficient (mol^{-1} dm^3 cm^{-1}).

Samples for powder X-ray diffraction (XRD) were separated from the suspensions by centrifugation and, after washing with pure water, they were dried at 60°C for 2 d under vacuum. The XRD data of the samples were collected at $2\theta = 1.5°–30°$ at a scan speed of 1.0 cm/min using a Rigaku RINT-2000 powder diffractometer, with Ni-filtered CuK radiation. The amount of dyes in each sample was determined by the elemental analysis for carbon, hydrogen, and/or nitrogen.

RESULTS AND DISCUSSION

Absorption spectra of cationic dyes in aqueous solution

Metachromasy of cationic dyes in the aqueous solutions is commonly observed. The monomer band of CN-0 occurs at 520 nm with a secondary peak at 490 nm, which is caused by the vibrational actions of the dye molecule (Figure 2). In the dilute-concentration region, $<10^{-5}$ mol dm^{-3}, the absorption spectra of CN-0 did not show significant differences. However, the spectrum of a 2.0×10^{-4} mol dm^{-3} solution showed a slight absorption band of *J*-aggregates at 570 nm and the shift of the peak at ~490 nm to shorter wavelength by the appearance of the dimer band at 480 nm. On addition of KBr into the aqueous solution of 10^{-4} mol dm^{-3}, where KBr induces an apparent increase of the dye concentration, spectral differences (Figure 3) were observed by the decrease of the *M* band at 520 nm and the increase of the *J* band at 570 nm. The characteristic *J* band of CN-0 occurred in concentrated aqueous solutions and in aqueous solutions with salts.

https://doi.org/10.1346/CCMN.2000.0480310 Published online by Cambridge University Press

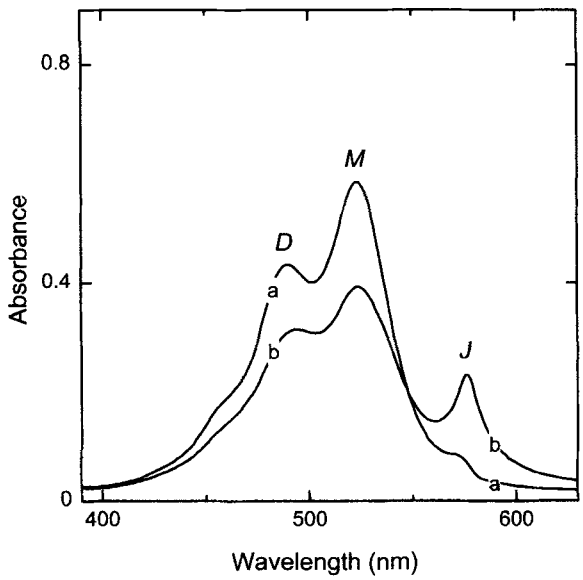

Figure 3. Absorption spectra of CN-0 in aqueous solutions for a concentration of 1.0×10^{-4} mol dm^{-3} and KBr concentrations of (a) 0.04 mol dm^{-3} and (b) 0.4 mol dm^{-3}. Optical path length: 1 mm.

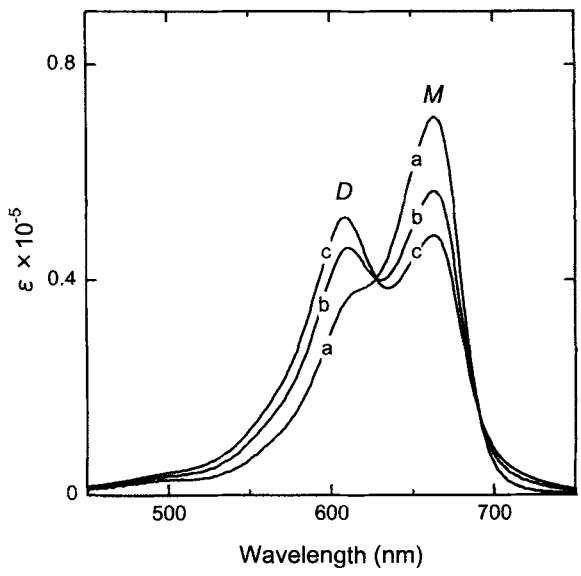

Figure 4. Absorption spectra of MB in aqueous solutions. Curve (a) shows the spectrum for a concentration of 1.0×10^{-5} mol dm^{-3}, (b) for 1.0×10^{-4} mol dm^{-3}, and (c) for 2.5×10^{-4} mol dm^{-3}. ϵ is the molar absorption coefficient (mol^{-1} dm^3 cm^{-1}).

At extremely high concentrations, the intensity of the *M* band at 520 nm decreased and the *J* band occurred at 572 nm as a sharp peak. Daltrozzo *et al.* (1974) proposed four possible structures for *J*-aggregates and discussed the close relationship between crystallization and *J*-aggregation. Tanaka *et al.* (1980) studied the electronic spectra of single crystals of CN-0 to determine the origin of the *J* band. Yoshioka and Nakatsu (1971) showed by X-ray structural studies that two quinoline rings are twisted relative to each other, and each ring stacks with one quinoline ring of an adjacent molecule. The probable geometry of the *J*-aggregates is expected to be similar to that of the crystal structure. In contrast to the structure study, however, *J*-aggregation occurs in solution only where the slipping angle of adjacent monomer units is large and the dye distribution remains homogeneous in the solution (Sturmer and Heseltine, 1977).

MB in dilute solutions, $<1 \times 10^{-4}$ mol dm^{-3}, showed a maximum at 665 nm with a shoulder at 615 nm, labeled as *M* and *D* bands, respectively (Figure 4). More concentrated solutions, 2.5×10^{-4} mol dm^{-3}, showed a change in the relative intensity of the two bands with the *D* band greater than the *M* band. A further increase in concentration resulted in a broader band near 600 nm. The metachromasy of aqueous MB solutions may be related to the formation of dimers and *H*-aggregates. The molecules forming a dimer unit are probably bonded by π-π interactions and hydrophobic interactions (Tanford, 1980) which overcome the electrostatic repulsion between the positive charges of each MB molecule (Bergmann and O'Konski, 1963). The interaction between molecules should be greatest when the monomer units are in a "sandwich-like" structure with the principal molecular axes being parallel. The coulombic repulsion is much lowered where the charged amino groups lie along the opposite edges of the sandwich. The stacked sandwich structure is the most stable for the higher aggregates.

Similarly, the main band in the absorption spectra of propeller-shaped CV was split into two parts, the *M* band at 590 nm and *D* band at 550 nm. The relative intensity of the *M* and *D* bands varied with the dye concentration (Schubert and Levine, 1955; Stork *et al.*, 1972; Takatsuki, 1980). At moderately high concentration, the spectral change showed an enhancement of the *D* band and a diminution of the *M* band. When the dye concentration was increased further, both *M* and *D* bands were depressed and aggregate bands (*H*-aggregates) occurred, which appeared on the shorter wavelength side of the *D* band. A "sandwich-like" structure for CV dimers is also preferable as well as for MB to minimize the energy of association.

The absorption spectra of the two cyanine dyes in the mixture of ethanol and water showed a peak at 605 nm for CN-1 and a 709-nm peak for CN-2. The effect of the dye concentration on the absorption spectra of CN-1 and CN-2 did not show appreciable changes in the concentration range of $<10^{-5}$ mol dm^{-3}. In aqueous solution, however, CN-1 showed a notable *D* band at 560 nm in this concentration range (Iwasaki *et al.*, 1992).

https://doi.org/10.1346/CCMN.2000.0480310 Published online by Cambridge University Press

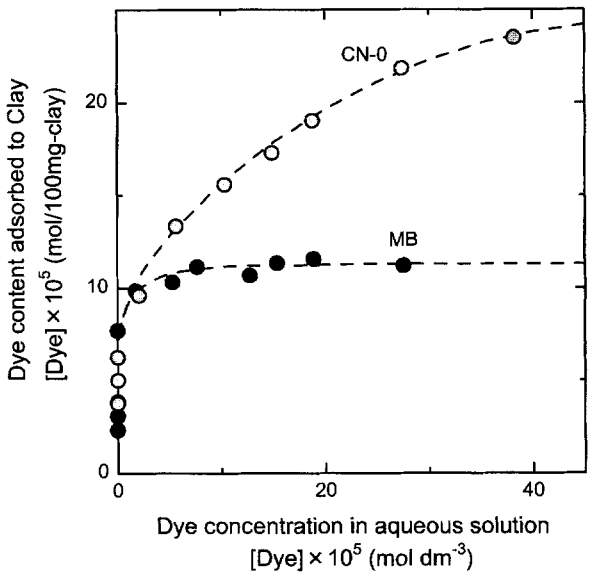

Figure 5. Adsorption isotherms of MB (●) and CN-0 (○) for saponite clay at 25°C.

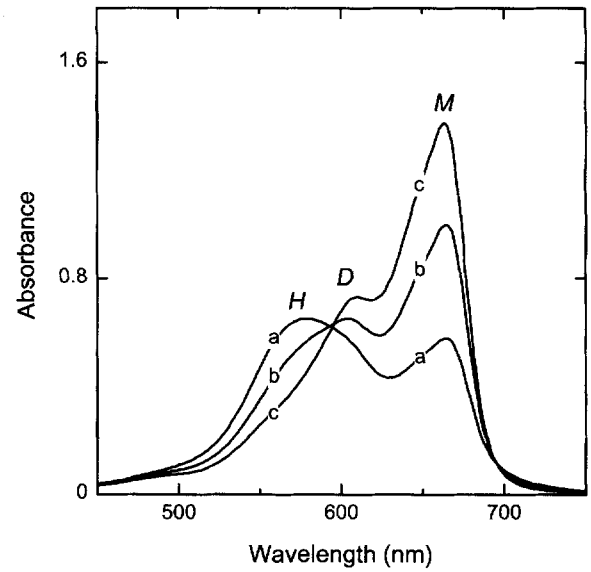

Figure 6. Absorption spectra of MB in clay suspensions for a concentration of 2.0×10^{-5} mol dm^{-3}. Clay concentrations: (a) 40 mg dm^{-3}, (b) 70 mg dm^{-3}, (c) 120 mg dm^{-3}. Optical path length: 1 cm.

Effect of synthetic saponite on absorption spectra of cationic dyes

The adsorption of cationic dyes in synthetic saponite occurs by a cation-exchange reaction. Exchangeable metal cations (Na^+) are simultaneously released into aqueous solution when dyes are intercalated into the clay. The adsorption isotherms for MB and CN-0 are shown in Figure 5, where the dye content adsorbed in the clay is plotted against equilibrium concentration of the dye in solution. Whereas the adsorption of MB was saturated at 113 mmol/100 g-clay, corresponding to the CEC value of saponite, the amount of CN-0 adsorbed increased beyond the CEC value following Freundlich-type adsorption. This result suggests the contribution of physical adsorption in addition to ionic adsorption for intercalation of CN-0 in the clay.

The effect of an increment of the clay on the absorption spectra of the dye was studied. The dye solution with a small amount of the clay showed a change in color. In such suspensions, the interlayer of the clay is saturated with some dye molecules and other molecules remain in the solution. After filtration through the membrane film, the filtrate showed the characteristic spectrum of the free dye. When the amount of clay in suspension was increased, free-dye molecules were adsorbed in the clay and floating flocculates were observed. The filtrates of these suspensions were transparent and showed no absorption in the visible range. On further increase of the clay amount, the dye molecules uniformly adsorbed in the clay and the dye-clay complexes were distributed homogeneously in suspensions. The absorption spectra of such dye-clay suspensions resembled that of the dilute dye solution. Figure 6 shows the visible spectra of MB in aqueous suspensions with saponite. The supernatants of these suspensions were transparent. The broad peak at ~570 nm (Figure 6, curve a) appeared at high loading of MB and corresponded to *H*-aggregates, whereas the spectrum at low loading resembled that of the MB monomer in dilute aqueous solution (Figure 6, curve c). This result suggests that most MB molecules can exist as monomers on the clay in suspensions of low loading. Similar effects were also reported for planar acridine orange (Cohen and Yariv, 1984) and pyronin Y (Grauer *et al.*, 1987), both of which resemble MB in molecular shape.

The adsorption of CV in saponite produced a slight metachromasy similar to that observed for MB. CV in suspensions of low loading showed an absorption band with an intensity maximum at 590 nm, whereas at higher loadings of CV, the absorption band shifted to shorter wavelength with the decrease of the *M* band, indicating the formation of dimers and higher aggregates of CV. These results correspond to the spectral changes of adsorption of CV to Laponite and montmorillonite studied by Yariv *et al.* (1990). Similarly, the absorption bands of CN-1 and CN-2 in the dye-clay suspensions were wider and shifted to shorter wavelength, *i.e.*, to 470 and 520 nm, respectively, with the decrease of the respective *M* bands, when compared to those in aqueous solutions.

Figure 7 shows the absorption spectra of suspensions of CN-0 and saponite with different clay concentrations. Note that the spectra differ from those of MB-saponite suspensions. Small amounts of saponite

https://doi.org/10.1346/CCMN.2000.0480310 Published online by Cambridge University Press

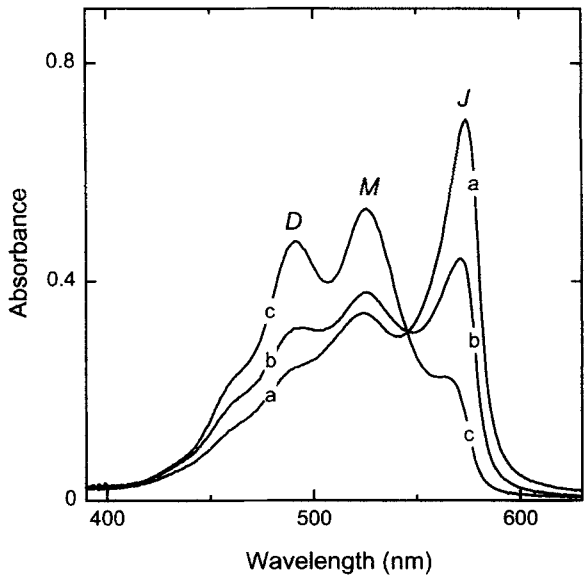

Figure 7. Absorption spectra of CN-0 in clay suspensions for a concentration of 1.0×10^{-5} mol dm^{-3}. Clay concentrations: (a) 5.0 mg dm^{-3}, (b) 7.5 mg dm^{-3}, (c) 11.5 mg dm^{-3}. Optical path length: 1 cm.

in the CN-0 solution produce a significant band (*J*) at 573 nm (Figure 7, curve a). Further increases in the amount of the clay gradually increases the intensity of the *M* band, because the interaction of the dye molecules in the interlayer decreases (Figure 7, curve c) owing to fewer molecules per unit area in the interlayer. These results suggest that CN-0 has a tendency to form *J*-aggregates in the interlayer of saponite. The absorption bands of dye-clay suspensions are summarized in Table 1.

Table 2. Calculated size of dye molecules.

Dye	Width (W)	Height (H)	Length (L)	(H − W)
MB	4.7	7.9	16.4	3.2
CV	6.1	15.0	16.5	8.9 (10.4)[1]
CN-0	5.3	9.7	16.9	4.4
CN-1	5.1	9.6	19.3	4.5
CN-2	5.1	9.5	22.3	4.4

[1] The value in parentheses is (L − W), see text.

Orientation of cationic dyes intercalated in saponite

The most stable molecular structure of each cationic dye was determined by means of MOPAC (Molecular Orbital Package) computation and AM1 (Austin Model 1) theory (Dewar, 1985) to minimize the energy of the dye molecule. The computation was performed with a molecular modeling application, CS chem3D, from CambridgeSoft Corp. (Cambridge, Massachussetts, USA), and applied only for a free molecule and not for dimers and aggregates. The three planar dyes, MB, CN-1, and CN-2, are flat chromophores, and the non-planar dyes, CV and CN-0, have twisted conformations, *e.g.,* the twist angle between the two quinoline planes of CN-0 is 47°. The calculated sizes of each dye molecule are given in Table 2 and the space-filling models for MB and CN-0 are illustrated in Figure 8. The preferable molecular structure of MB has the size of 4.7 (width, W), 7.9 (height, H), and 16.4 Å (length,

Table 1. Basal spacing [*d*(001), Å] of dye-saponite complexes with adsorbed amount of dye, and absorption bands of their respective suspensions.

Dye		Low Loading				High Loading
MB	*d*(001)	13.2	13.4	13.6	14.7	15.5
	Adsorbed amount (mmol/100 g-clay)	19.1	29.2	65.2	98.5	135.1
	Absorption band (nm)	*M* at 665 ≫ *D* at 615			broad *H* (*D*) at 570 > *M* at 670	
CV	*d*(001)	14.0	14.7	16.7	21.0	24.5
	Adsorbed amount (mmol/100 g-clay)	10.0	19.0	39.5	58.0	75.8
	Absorption band (nm)	*M* at 590 ≫ *D* at 550			broad *H* (*D*) at 540 > *M* at 590	
CN-0	*d*(001)	14.3	16.4	17.0	17.3	18.0
	Adsorbed amount (mmol/100 g-clay)	14.1	44.6	64.1	90.1	114.8
	Absorption band (nm)	*M* at 520			*D* at 480, *J* at 570 > *M* at 520	
CN-1	*d*(001)	13.8	14.2	16.7	17.7	18.4
	Adsorbed amount (mmol/100 g-clay)	14.8	25.9	52.4	71.3	95.8
	Absorption band (nm)	*M* at 610			broad *H* (*D*) at 500 > *M* at 610	
CN-2	*d*(001)	13.8	14.2	16.7	17.0	18.4
	Adsorbed amount (mmol/100 g-clay)	16.7	20.5	35.0	53.9	69.9
	Absorption band (nm)	*M* at 710			broad *H* (*D*) at 560 > *M* at 710	

≫ and > show the relative intensities between the absorption bands, they mean "much higher" and "higher", respectively.

https://doi.org/10.1346/CCMN.2000.0480310 Published online by Cambridge University Press

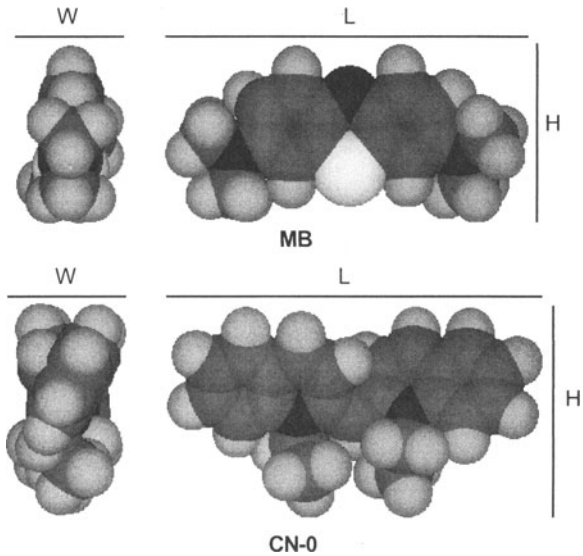

Figure 8. The space-filling models for MB and CN-0 determined by MOPAC computation. Width, height, and length are abbreviated as W, H, and L, respectively.

L). Non-planar CV and CN-0 were also estimated and, because of the deviation from planarity, gave a large width.

The untreated saponite showed a basal spacing [d(001)] of 12.6 Å by powder XRD. In this case, the observed basal spacing is the sum of the thickness (Δl) of a 2:1 layer and the diameter of the exchangeable hydrated-metal cation. Powder XRD patterns of dye-saponite complexes for CN-0 at various amounts of adsorbed dye are illustrated in Figure 9. The d(001) value for the dye-clay complex varies depending upon the amount of cationic dyes absorbed, as shown in Table 1 and Figure 10. The XRD data of the dye-clay complexes showed that the basal spacings expanded to >12.6 Å. The larger values of d(001) were obtained from samples with a higher degree of saturation of dyes, indicating that dyes were located in the interlayer. The interlayer gradually expanded with increasing dye content and approached a maximum value at near the CEC. At low loadings (<20 mmol dye/100 g-clay), the d(001) value was 13–14 Å for each of the five dyes. At high loadings near the CEC value, d(001) values for MB-clay and CV-clay complexes were ~16 and ~25 Å, respectively. For the complexes of CN-0, CN-1, and CN-2, the d(001) values were ~18 Å. The d(001) value varied with an increase in the absorbed amount and with the shape and the size of the dye used. The difference between the basal spacings for clays with high and low loading reflects the apparent variations in the orientation of dye molecules in the interlayer. These differences for each dye-clay complex were about 3, 11, and 4 Å for MB, CV, and three cyanine dyes, respectively. The estimated values of 3 Å and 4 Å for MB and three cyanine dye complexes

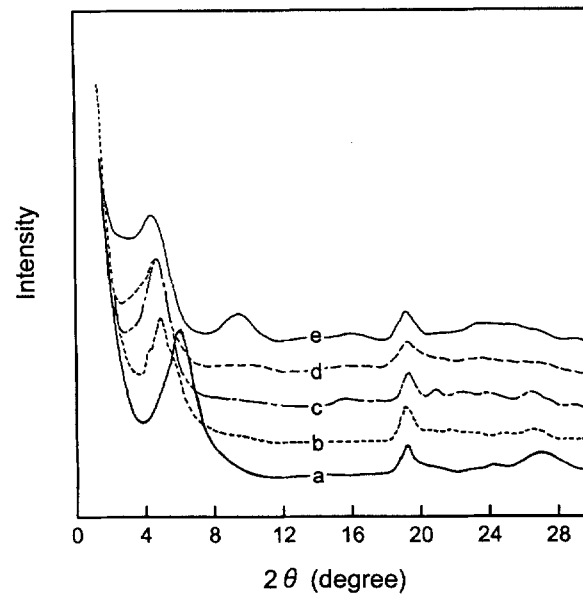

Figure 9. XRD patterns of CN-0-saponite complexes. Adsorbed amounts of CN-0 in 100 g clay: (a) 14.1 mmol, (b) 44.6 mmol, (c) 64.1 mmol, (d) 90.1 mmol, (e) 114.8 mmol. Basal spacings of respective complexes are listed in Table 1.

correspond to the respective differences (H − W) of the height and the width of dye molecules, as listed in Table 2. The value of 11 Å for the CV-clay complex, was much closer to that (L − W) of the length and the width of a CV molecule. CV molecules are likely to interact with each other vertically with a 60° rotation to reduce steric hindrances.

To estimate the thickness of a 2:1 layer (Δl), an appropriate size of a dye molecule was subtracted

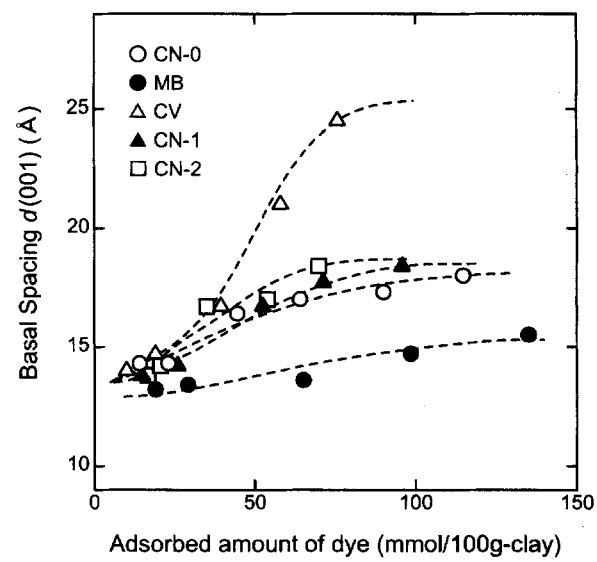

Figure 10. Basal spacing of dye-saponite complexes varied with the adsorbed amount of dyes.

https://doi.org/10.1346/CCMN.2000.0480310 Published online by Cambridge University Press

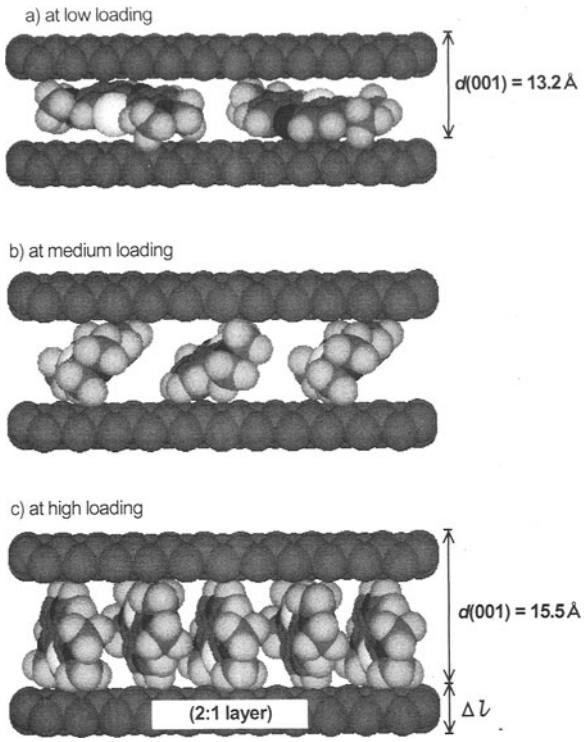

Figure 11. Orientation of MB intercalated in the dye-clay complex, a) at low loading, b) at medium loading, c) at high loading. Δl represents the 2:1 layer thickness. The 2:1 layer is drawn schematically.

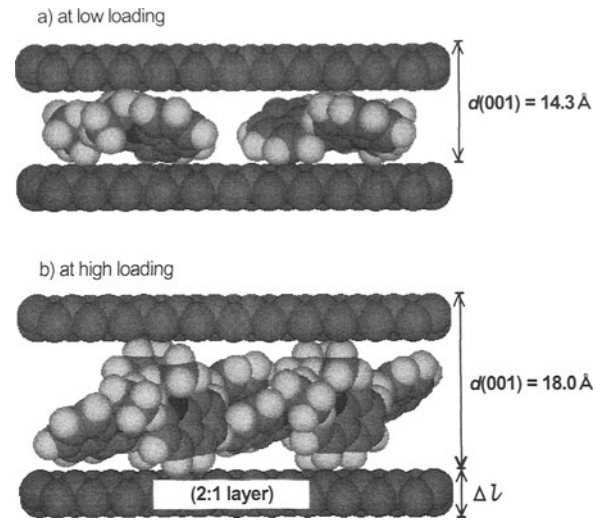

Figure 12. Probable intercalated alignment of CN-0 in the dye-clay complex, a) at low loading, b) at high loading. Δl represents the 2:1 layer thickness. The 2:1 layer is drawn schematically.

from the measured basal spacing, $d(001)$. The estimated value was 8.6 ± 0.4 Å by subtracting each width of five dye molecules from the corresponding $d(001)$ at low loading, and assuming that the dye molecules are lying flat between adjacent layers. At high loading, near the CEC value, a similar calculation by subtracting each height gave 8.6 ± 0.9 Å, where the orientation of dye molecules is assumed to occur vertically to the layers. Regardless of the different shape and size of the dye molecules and the variable loads up to the CEC, a consistent value was obtained for Δl. The $d(001)$ values suggest that the orientations change from horizontal at low loadings to vertical at high loadings of dye molecules between the 2:1 layers.

Note that the 2:1 layer thickness of 8.6 Å differs from the unit-cell spacing of 9.6 Å common to talc or pyrophyllite because it does not include the interlayer region between adjacent layers. In summary, 1) these dyes are oriented flat, *i.e.,* lying with their π planes parallel to the clay surface at low loading, 2) tilt towards the vertical (*i.e.,* c^* axis) with an increase in dye saturation, and 3) stand vertically to the clay surface at high loading, as illustrated in Figure 11. In Figures 11 and 12, two 2:1 layers and an interlayer with dye molecules are illustrated for each condition. Although such structures for the dimer and the aggregates could not be determined by the computations, as noted above, the arrangements of the planar dye molecules with aromatic ring(s) in the interlayer are reasonably modeled. These models use the thickness of a 2:1 layer, Δl, and simple assumptions that the dye molecules are plate-like and may be represented by width, height, and length values, and that they have maximum contact with neighboring molecules owing to π-π interactions. The geometry of aggregates in the interlayer is also described based on the sandwich structure of the MB dimer (Bergmann and O'Konski, 1963). The favorable π-π interactions and balanced electrostatic interactions of the cationic dye molecules are produced by the alternating vertical orientation as shown in Figure 11c instead of any combination of stacking of horizontal molecules. Similar results for protonated tetramethyl benzidine on hectorite were reported by McBride (1985). Such a topology permits the adsorption of colored benzidine as monomeric cations with an orientation that is horizontal to the surface, followed by intercalation of the cations as paired species oriented vertically to the surface.

The specific cationic cyanine dye, CN-0, has a twisted chromophore with a dihedral angle of 47° owing to the steric hindrance between the hydrogen atoms at the 3,3′-position. The spectrum at the highest-loading conditions shows a marked *J* band (*e.g.,* Figure 7, curve a). The relative amount of CN-0 at which the marked *J* band occurred, was higher than the CEC value, which differs from these cases of the *H*-aggregates of the other dyes. The basal spacings in Table 1 varied from 14 to 18 Å showing the spectral change from the *M* band to the *J* band. Daltrozzo *et al.* (1974) proposed the models for *J*-aggregates of CN-0. Be-

https://doi.org/10.1346/CCMN.2000.0480310 Published online by Cambridge University Press

cause of the inherent asymmetry of the twisted chromophore, CN-0 forms *J*-aggregates in at least three different ways: a) aggregates with alternating antipodes (non-helical), b) clockwise, and c) counterclockwise helical configurations consisting of only one type of antipode. Proposed interlayer alignments of CN-0 in dye-clay complexes at low and high loading are illustrated in Figure 12. A non-helical model is given for aggregates (Figure 12b) because of the achiral environment of the saponite layer. This model is preferred in that the orientation is more stable when the π planes of adjacent molecules are parallel to each other and the positively charged nitrogen atoms are on the opposite edges.

ACKNOWLEDGMENT

The authors are grateful to the reviewers for helpful comments, and wish to thank S. Guggenheim and L. Ukrainczyk for important suggestions and remarks.

REFERENCES

Bergmann, K. and O'Konski, C.T. (1963) A spectroscopic study of methylene blue monomer, dimer, and complexes with montmorillonite. *Journal of Physical Chemistry,* **67,** 2169–2177.

Breen, C. and Rock, B. (1994) The competitive adsorption of methylene blue on to montmorillonite from binary solution with thioflavin T, proflavine and acrydine yellow, steady-states and dynamic studies. *Clay Minerals,* **29,** 179–189.

Carroll, B.H., Higgins, G.C., and James, T.H. (1980) *Introduction to Photographic Theory, The Silver Halide Process.* John Wiley & Sons, New York, 160–195.

Cenens, J. and Schoonheydt, R.A. (1988) Visible spectroscopy of methylene blue on hectorite, Laponite B, and barasyn in aqueous suspension. *Clays and Clay Minerals,* **36,** 214–224.

Chernia, Z. and Gill, D. (1999) Flattening of TMPyP adsorbed on Laponite. Evidence in observed and calculated UV-vis spectra. *Langmuir,* **15,** 1625–1633.

Cohen, R. and Yariv, S. (1984) Metachromasy in clay minerals, Acridine orange by montmorillonite. *Journal of the Chemical Society, Faraday Transaction 1,* **80,** 1705–1715.

Daltrozzo, E., Scheibe, G., Gschwind, K., and Haimerl, F. (1974) On the structure of the J-aggregates of pseudoisocyanine. *Photographic Science and Engineering,* **18,** 441–450.

Dewar, M.J.S., Zoebisch, E.Z., Healy, E.F., and Stewart, J.J.P. (1985) AM1: A new general purpose quantum mechanical molecular model. *Journal of the Chemical Society,* **107,** 3902–3909.

Duxbury, D.F. (1995) Photochemistry and photophisics of triphenylmethane dyes in solid and liquid media. *Chemical Review,* **93,** 381–433.

Grauer, Z., Grauer, G.L., Avnir, A., and Yariv, S. (1987) Metachromasy in clay minerals, sorption of pyronin Y by montmorillonite and Laponite. *Journal of the Chemistry Society, Faraday Transaction 1,* **83,** 1685–1701.

Hang, P.T. and Brindley, G.W. (1970) Methylene blue absorption by clay minerals. Determination of surface areas and cation exchange capacities (clay-organic studies XVIII). *Clays and Clay Minerals,* **18,** 203–212.

Ito, K., Zhou, N., Fujiwara, Y., and Fukunishi, K. (1994) Potential use of clay-cationic dye complex for dye fixation in thermal dye transfer printing. *Journal of Imaging Science and Technology,* **38,** 575–579.

Ito, K., Kuwabara, M., Fujiwara, Y., and Fukunishi, K. (1996) Application of clay-cationic dye intercalation to image fixation in thermal dye transfer printing. *Journal of Imaging Science and Technology,* **40,** 275–280.

Iwasaki, M., Kumagai, M., and Tanaka, T. (1992) Dissociation equilibrium of bimolecular associates of 2,2′-carbocyanine. *Journal of the Chemical Society of Japan,* **1992,** 1052–1056. (in Japanese).

Jelley, E.E. (1936) Spectral absorption and fluorescence of dyes in the molecular state. *Nature,* **138,** 1009–1010.

McBride, M.B. (1985) Surface reactions of 3,3′,5,5′-tetramethyl benzidine on hectorite. *Clays and Clay Minerals,* **33,** 510–516.

Ogawa, M. and Kuroda, K. (1995) Photofunctions of intercalation compounds. *Chemical Review,* **95,** 399–438.

Ogawa, M., Kawai, R., and Kuroda, K. (1996) Adsorption and aggregation of a cationic dye on smectites. *Journal of Physical Chemistry,* **110,** 16218–16221.

Saehr, D., Le Dred, R., and Hoffner, D. (1978) Study of vermiculite-cationic dye interactions. *Clay Minerals,* **13,** 411–425.

Schoonheydt, R.A. and Heughebaert, L. (1992) Clay adsorbed dyes: Methylene blue on Laponite. *Clay Minerals,* **27,** 91–100.

Schubert, M. and Levine, A. (1955) A qualitative theory of metachromasy in solution. *Journal of the American Chemical Society,* **77,** 4197–4201.

Stork, W.H.J., Lippits, G.J.M., and Mandel, M. (1972) Association of crystal violet in aqueous solutions. *Journal of Physical Chemistry,* **76,** 1772–1775.

Sturmer, D.M. and Heseltine, D.W. (1977) Sensitizing and desensitizing dyes. In *The Theory of the Photographic Process, 4th edition,* T.H. James, ed., Macmillian, New York, 218–222.

Takatsuki, M. (1980) Quantitative study of metachromasy. The analysis of the dye polyphosphate multi equilibrium system of the principal component analysis method. *Bulletin of the Chemical Society of Japan,* **53,** 1922–1930.

Tanaka, T., Tanaka, M., and Hayakawa, M. (1980) Electronic spectra of single crystals of 1,1′-diethyl-2,2′-cyanine iodide, bromide, and chloride. *Bulletin of the Chemical Society of Japan,* **53,** 3109–3119.

Tanford, C. (1980) *The Hydrophobic Effect, 2nd edition.* Wiley-Interscience, New York, 233 pp.

Yariv, S., Nasser, A., and Bar-on, P. (1990) Metachromasy in clay minerals, Spectroscopic study of the adsorption of crystal violet by Laponite. *Journal of the Chemical Society, Faraday Transaction,* **86,** 1593–1598.

Yoshioka, H. and Nakatsu, K. (1971) Crystal structure of two photographic sensitizing dyes, 1.1′-diethyl-2,2′-cyanine bromide and 1,1′-diethyl-4,4′-cyanine bromide. *Chemical Physics Letters,* **11,** 255–258.

E-mail of corresponding author: fuku@ipc.kit.ac.jp

(Received 1 July 1999; accepted 26 February 2000; Ms. 357; A.E. Ljerka Ukrainczyk)